The Impact of Gravitational Waves: Detectability and Signatures

Jenna Klemkowsky
Wheeling Jesuit University

Summer 2013
University of Florida
International Research Experience for Undergraduates

University of Birmingham
Gravitational Waves Group
Mentors: Alberto Vecchio, Ilya Mandel, and Kat Grover

ABSTRACT

Gravitational waves have provided a major push in improving the ground-based detectors, especially since there is hope that detections can be made within the upcoming years. In order to prepare for these possible detections, there is a lot of ongoing research being done to keep the astrophysical and detection information as current as possible. This project was designed to play into this demand by updating the current calculator made by the Gravitational Wave Group at the University of Birmingham, which is used to simulate detections of gravitational waves. Not only have these changes been made to keep the calculator up-to-date with the most recent research for LIGO and the interested public, but it has also provided some interesting comparisons and results that can be further explored.

INTRODUCTION

Advancements in the ground-based detectors, including the Laser Interferometer Gravitational-wave Observatory (LIGO), have led to the hopes of detections of gravitational waves (GWs) being made within the next few years.[1] As this time frame approaches, it is important that up-to-date astrophysical data be used in both predicting the number of GW signals Advanced LIGO (aLIGO) will detect and in understanding the number of detections once aLIGO is online. Through simulations of GW sources and detectors, there is a high level of complexity being used in order for these predictions and potential understandings to be made possible. This creates a need for an event rate calculator the can use the most recent astrophysical information as well as the most current expectations of the form of gravitational wave signals and sensitivities, both of which are discussed further in the background. Since there are still several uncertainties in these predictions, the ability to continuously change the inputs to reflect the latest models is crucial in making sure the computations being implemented are as realistic as possible.

There already exists a calculator developed by the GW Group at the University of Birmingham for LIGO and interested public to use as an online tool, but it is necessary to expand upon what had already been developed. This calculator can be seen at the following website: http://www.sr.bham.ac.uk/gwastro/rates. The purpose of this current project is to make the appropriate expansions while also making the calculator as physically correct as possible. These all need to be done while keeping in mind that these calculations need to be made fast enough to run on a website.

BACKGROUND

The number of detections made by GW detectors depends on three types of parameters: the detectors and their sensitivity, the types of signals being received, and the astrophysical distribution of the GW sources.

1. DETECTORS

The first generation detectors, LIGO found in the United States, VIRGO found in Italy, and GEO600 found in Germany, have produced astrophysically interesting results.[2] These results have provided a better understanding of placing limits on GW sources as there have been no true GW detections made thus far. The major improvement to the detectors is finding a way to decrease the amount of background noise being received by these detectors. The data being collected by the detectors is a sum of the background noise and the GW signals.

From Earth, the strength of the weakest signals that can be detected and the distance that this source can be seen is determined by how much noise there is within the detector.[3] In order to receive the best results and although they can never be fully eliminated, these principal noise sources must be lowered, which vary depending on the frequency range. It is predicted that by 2015, the advancements made to the detectors will make the sensitivity ten time greater, which makes the detection volume increase by a factor of one thousand.[4] Figure 1[5] shows these anticipated contributions from sources in a single aLIGO detector compared to the detectors total sensitivity.

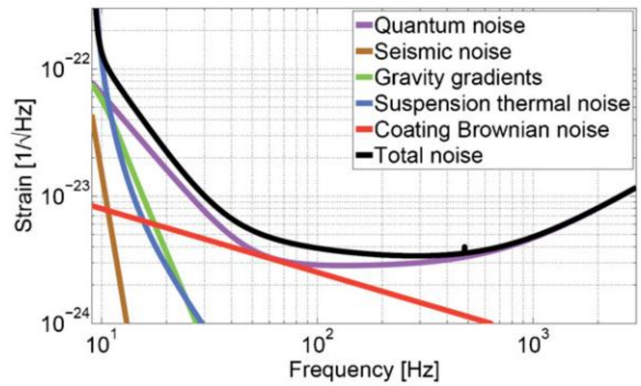

Figure 1: Estimated contributions from individual noise sources to the total aLIGO sensitivity.

2. WHERE WILL THESE DETECTIONS COME FROM?

The rates calculator is only currently concerned with Compact Binary Coalescences (CBCs), which deem to be the most promising sources. Part of what aLIGO will hopefully detect are inspirals, mergers, and ringdowns of GWs associated with the merging of compact binary systems made of neutron starts (NSs) or black holes (BHs).[6] CBCs are known for being very clean sources of gravitational waves due to the fact that it's waveforms are highly accurate yet only determined by a small amount of parameters, which include: the source's location, orientation, time of coalescence, and orbital phase at coalescence, as well as the bodies' masses and angular spin momenta.[7] In implementing these parameters, observers will be able to accurately compare actual waveforms of the GWs collected from the detectors to the theoretically derived templates. The exact form of GWs from CBCs in some instances has been calculated using numerical relativity, but in genereal these theoretical approximants must be relied upon. There are a variety of ways these approximations can be generated whether it is in using the time or frequency domains, or including merger and ringdown parts of the objects, all of which leads to various different waveform approximants that can be used in simulations and data analysis.[8] Once aLIGO is complete, although this must be stressed that this is an estimate using a particular astrophysical model, it is estimated to detect 40 neutron star inspiral events per year, 10 solar massed black hole binaries is 30 per year, and 10 per year for mixed neutron star-black hole inspirals. [9]

It must be kept in mind that out of these three mass systems being explored; neutron star binaries are the only types that have been directly observed. This evidence comes from galactic binary pulsars, which are double NS systems that has one of the NSs being a pulsar.[10] The other two types of systems, black hole binaries (BBHs) or one black hole and one neutron star (NS-BH), have not been observed, which only allows us to make predictions and rely heavily on different types of models for both forms of the waves and the number of mergers. In using these various models, it will be necessary to incorporate all the parameters so that these theoretical results can be compared to potential detection results because GW detections are the only way to study that mass systems.

3. Signal to Nose Ratio

Another way to increase the chance of making detections, there can also be improvement in the signal-to-noise ratio (SNR) from any signals received from the three possible CBCs. This ratio is crucial in being able to understand over what range of frequency and with what amount of detector noise will allow gravitational wave detections to be made. Equation 1[11],

$$\rho = \sqrt{4 \int_0^{f_{ISCO}} \frac{|h(f)|^2}{S(f)} df}, \tag{1}$$

shows the calculation of the SNR for a single detector, where h(f) is the frequency-domain waveform amplitude, f_{ISCO} is the frequency of the innermost stable circular orbit of the GW from the binary (this is not the frequency of the binary), and S(f) is the noise power spectral density (PSD), which is the characteristic noise of the detector. It must be mentioned that this is a very conservative calculation since it only includes the inspiral portion of the waveform. The merger and ringdown parts are ignored because they will not play a crucial role in the SNR for low-mass binaries.[12]

The detector is most sensitive to the signals with the highest SNR. An SNR threshold of 8 is a value usually chosen to claim a detection, which is based on the approximation that the detector noise is Gaussian, meaning how we describe the random noise, and stationary, meaning the noise at one moment in time is uncorrelated to the noise at another moment. In keeping this fiducial threshold SNR, the distance we can go out in order to make these detections, which is called the optimal horizon distance, can now be explored. This distance relates to this ratio through observing proportional relationships. The waveform amplitude, h, is proportional to 1/distance, so based on the formula given in Equation 2, the SNR has this same proportionality. As a part of this current project, the optimal horizon distance is one of the things trying to be calculated, so it is important to keep in mind that any estimates/comparisons being made are based on particular astrophysical models and the most optimistic detector sensitivities.

Comparing LIGO to aLIGO, along with using 8 for the SNR threshold, there is quite a significant change in the horizon distance that can be assumed. For the initial LIGO, the horizon distances for NS-NS/BH-BH/NS-BH are 33 Mpc/ 70 Mpc/ 161 Mpc respectively, but for aLIGO these distances become 445 Mpc/ 927 Mpc/ 2187 Mpc.[13] It must be kept in mind again that these estimates are very rough, and it must also be known that the effects of redshift are not incorporated in these values. The use of redshift in these instances is only a way to step out in shells of distance to increment the calculations. In other calculations, there is also the usage of cosmological redshift as a way of incorporating the variation of certain values depending on what distance it is away from the local universe, which is used in the discussion later on.

4. ASTROPHYSICAL PARAMETERS

Astrophysical parameters are also important to keep in consideration when trying to determine the possibility of GW detections. One area that is significant to take a look at is the merging rate of CBCs because it is a vital factor in predicting the detection rate of these systems. Once these detection rates can be determined, it will create a limit on the astrophysical models and parameters being implemented. The rate at which two CBCs come together is not fully understood, but in the simplest models being used, these rates are based on the assumption that they are proportional to the star formation rate in these galaxies. For spiral galaxies like the Milky Way, these rates are tracked by using blue-light luminosity, but this rate fails to factor in a delay due to star formation of older elliptical galaxies for these mergers.[14] Merger rates can be more naturally evaluated as more studies begin to be published, but with the current information being used, these assumptions are useful for scaling observations. It must just be noted that this method can also alter the data for particular CBCs.

5. THE EXISTING CALCULATOR

The current calculator being implemented on the gravitational wave website through the University of Birmingham can be seen below in Figure 2. It allows the user to make selections based on the information they have, but it is limited in its' accuracy. This is simply because there aren't a lot of parameters being used to help make these predictions, and it isn't up-to-date with the most recent astrophysical information. If it doesn't stay updated then it won't allow realistic results to be observed, thus eliminating the website's true purpose.

In a little further detail, it can be seen that the merger rate being used is currently constant, one mass system can be used at a time, and a time-domain waveform must be selected. While these are all necessary concepts to take into account, it is better to expand upon them within the calculator, which is the main intention of this summer project as explain in the improvements section.

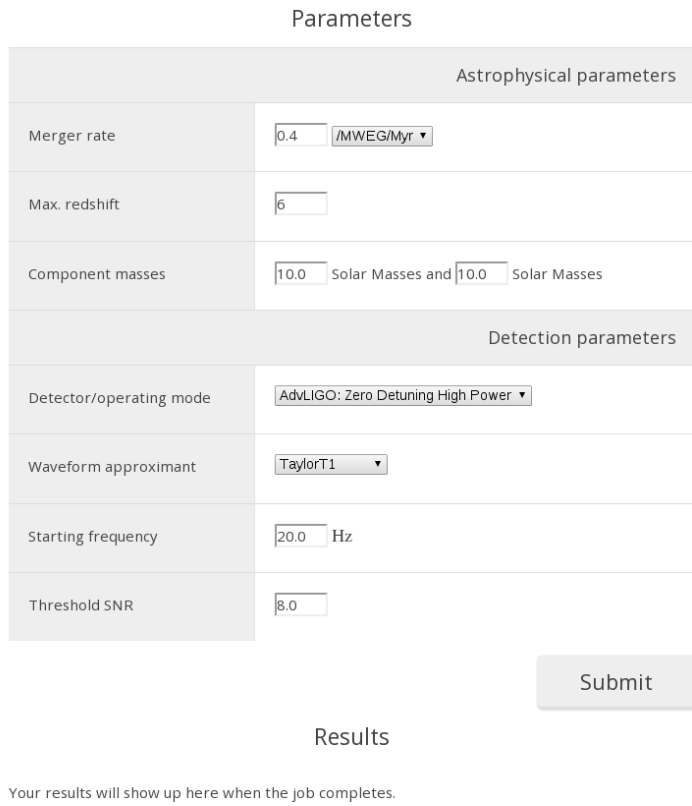

Figure 2: The gravitational wave event rate calculator before improvements were made

In order to understand the improvements being made, it is important to know the general existing algorithm of the calculation going on within the calculator. After the user selects the parameters for the CBC waveforms, the LIGO Algorithm Library (LAL) generates the waveform. In order for the waveform to be implemented properly, it must be in the time-domain, so if the waveform is currently in the frequency-domain, then a Fast Fourier Transform (FFT) will be used to make this conversion. Starting at a redshift of z=0, the calculations are made as we step out in each redshift shell. At these distances, the waveform is scaled for distance and redshift effects, and the SNR is also calculated at this distance. If this SNR is above the SNR threshold, the volume of this shell can be calculated. Using this volume, we can then multiply it by the given constant rate per volume and add to the total number of detections. This is all done by taking into account an isotropic distribution of binary locations and orientations. This process continues until the SNR threshold is reached or exceeded, which will terminate the calculations. Once complete, the user will receive the results in a table, which will show them the number of detections, the horizon redshift, the commoving distance, the time-domain waveform and frequency-domain waveform plots, the noise amplitude spectral density plot, and the SNR dependence on redshift plot.

IMPROVEMENTS

The overall purpose of this calculator is to provide a way for scientists or anyone interested from the public to be able to use for quick results and easy comparisons. In order for this is be done and for it to be realistic to the user, there were many improvements needing to be made to the initial calculator. The fact that there is still so much uncertainty in how many detections aLIGO will make, being able to alter the parameters in as many ways as possible will allow for justifications to be made in aLIGO's usefulness. Figures 3 and 4 show all of the additions made to the astrophysical and detection parameters, all of which will be explained in further detail below.

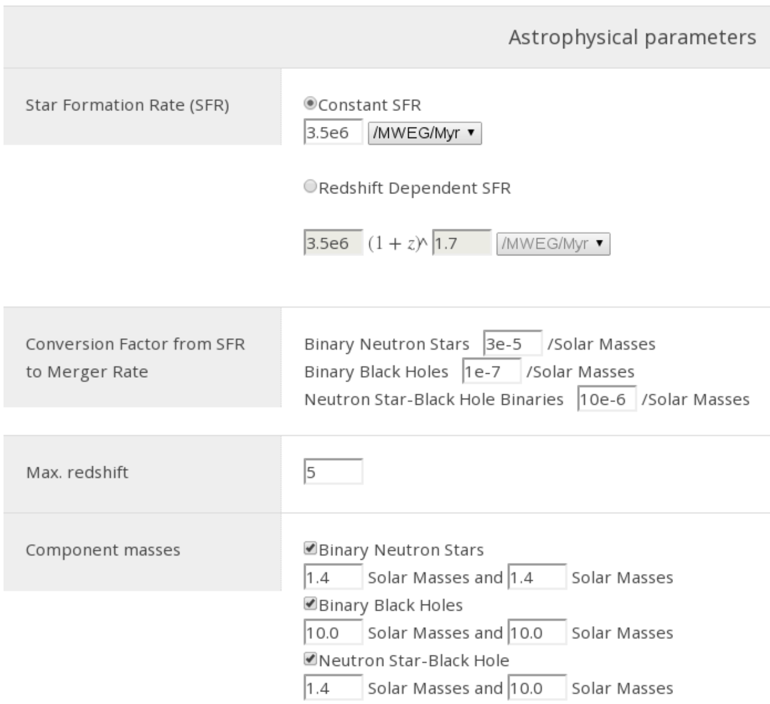

Figure 3: Updated astrophysical parameters on the GW event rate calculator.

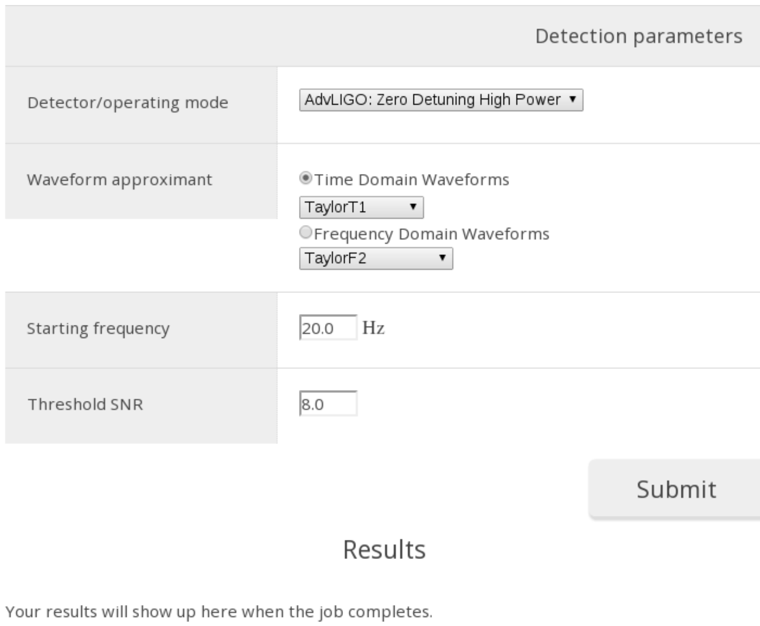

Figure 4: Updated detection parameters on the GW even rate calculator.

1. FREQUENCY WAVEFORMS

The first step in adding to the calculator was by adding in frequency-domain waveforms. The exact form of a detected GW cannot be perfectly modeled for all of the possible CBC sources, so it is important to use various models to compare the potential results. Figure 4 shows the changes made to this part of the calculator, which will allow the user to be able to easily select their preference of either a time-domain or frequency-domain waveform.

It is also important to understand that certain waveforms work better, faster, and/or more accurately with certain configurations of the detector. Although some of the waveforms in both domains output approximately the same results, it has been noticed that the frequency-domain waveforms calculate the result much more quickly. This is because in order to calculate the SNR, the frequency-domain waveform is needed, so it saves a lot of time if Fast Fourier Transform isn't needed to convert the time-domain waveform. Although this type of waveform saves time, it is sometimes thought that the time-domain forms are more accurate, so this option on the calculator will allow the user to decide the one they want.

In implementing this new option as a waveform, similar results can be seen between the TaylorT2 waveform and the TaylorF2 waveform, which is seen in Figure 5 with the rest of the input values remaining the same for each. This comparison between the two was just a check to show that this new result was quite similar to the original time-domain version.

Detection rate	159.2 per year
Detection rate BBH	13.5 per year
Detection rate BNS	36.7 per year
Detection rate NSBH	109 per year
Horizon redshift for BNS	0.1
Horizon redshift for BBH	0.5
Horizon redshift for NSBH	0.21
Comoving horizon distance BNS	416 Mpc
Comoving horizon distance BBH	1.89e+03 Mpc
Comoving horizon distance NSBH	852 Mpc

Detection rate	141.4 per year
Detection rate BBH	10.8 per year
Detection rate BNS	37.6 per year
Detection rate NSBH	93 per year
Horizon redshift for BNS	0.1
Horizon redshift for BBH	0.46
Horizon redshift for NSBH	0.2
Comoving horizon distance BNS	416 Mpc
Comoving horizon distance BBH	1.76e+03 Mpc
Comoving horizon distance NSBH	814 Mpc

Figure 5: Results for the TaylorF2 waveform (left) versus the TaylorT2 (right)

2. MULTIPLE MASS SYSTEMS

The next step was incorporating an option for the user to select more than one mass system at a time. GW detections in reality are expected to come from a wide range of masses, but for simplicity within the calculator, we split them into three main classes. This is important in being able to see how many detections can be made for the three different CBCs at the same time if the user chooses to do so. Figure 3 shows the way the improvements allow these options to be selected. Each mass system the user selects will show a result of how many detections are made within that class as well as adding it to the total number of detections.

3. STAR FORMATION RATES

The final incorporation to this calculator was the inclusion of redshift in the star formation rates (SFRs). This updated model will allow for a variable SFR, whereas the current calculator on allows a constant SFR. As stated previously, the merger rates we need in order to calculate the number of detections are scaled proportionally to the star formation rate. The most recent SFRs are discussed in articles by Steidel & Adelberger (see Figure 6)[15], who also based their rates off Equation 2, and Springel & Hernquist (see Figure 7)[16]. Based off these two models, a simpler more general fit was determined to scale as (1+z), which is the equation the user sees on the website. The user must input a value for the SFR_0, which is the SFR in the local universe, and an exponential value for (1+z).

The current calculator does not allow the user to select a conversion between the SFR and the merger rate which is a factor still highly unknown. In order to keep this area of the calculator updated, these values are still subject to change especially since the conversion isn't expected to be the same for the different massed CBCs. The conversion factors already placed in these areas are based off of the idea that there are approximately 3.5 solar masses per Milky Way Galaxy per year, and also by using the realistic merger rate values as seen in Figure 8 which vary for each binary system.

$$\dot{\rho}_{\star}(z) = \dot{\rho}_m \, \frac{\beta \exp\left[\alpha(z - z_m)\right]}{\beta - \alpha + \alpha \exp\left[\beta(z - z_m)\right]}, \tag{2}$$

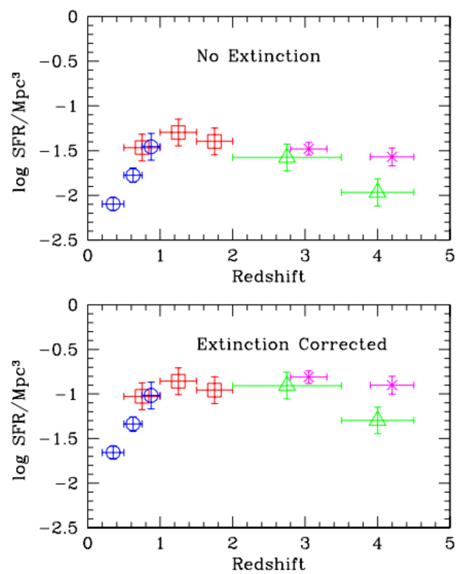

Fig. 9.— The UV luminosity density as a function of redshift, following Madau *et al.* 1996 (also using $H_0 = 50$ km s^{-1}Mpc^{-1} and $q_0 = 0.5$, for consistency). The different points come from Lilly *et al.* (1996) [circles], Connolly *et al.* (1997) [squares], and Madau *et al.* 1997 (triangles). The new points from this work are shown as crosses. See text for details.)

Figure 6: SFR calculations from the article by Steidel & Adelberger (with included caption from article).

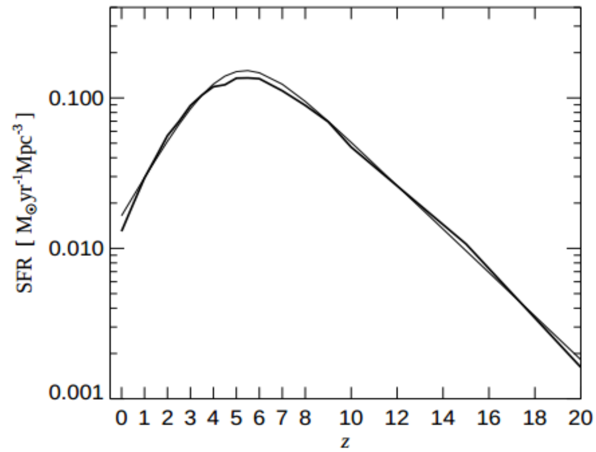

Figure 11. Cosmic star formation rate density of our composite simulation result (thick line) compared to the analytic fit (thin line) given in equation (14). The accuracy of the double-exponential fit is better than about 15% over the full redshift range $0 \leq z \leq 20$.

Figure 7: SFR based on article by Springel & Hernquist (with included caption from article).

TABLE II: Compact binary coalescence rates per Milky Way Equivalent Galaxy per Myr.

Source	R_{low}	R_{re}	R_{high}	R_{max}
NS-NS ($MWEG^{-1}$ Myr^{-1})	1 [1][a]	100 [1][b]	1000 [1][c]	4000 [16][d]
NS-BH ($MWEG^{-1}$ Myr^{-1})	0.05 [18][e]	3 [18][f]	100 [18][g]	
BH-BH ($MWEG^{-1}$ Myr^{-1})	0.01 [14][h]	0.4 [14][i]	30 [14][j]	
IMRI into IMBH (GC^{-1} Gyr^{-1})			3 [19][k]	20 [19][l]
IMBH-IMBH (GC^{-1} Gyr^{-1})			0.007 [20][m]	0.07 [20][n]

Figure 8: Estimated Rates of CBCs per MWEG.

In making this change to the calculator, there is already a significant observation to be made. This is the difference between a constant and a varying SFR while the same waveform is being used as well as all the other input data values. This is especially seen in the plot of the number of detections being made in relation to redshift, which is seen in Figure 9. Although the distance these detections are being measured out to remains the same, this clearly shows that when the effects of redshift being implemented within the SFR are taken into account, there is a higher amount of detections being made for certain CBCs.

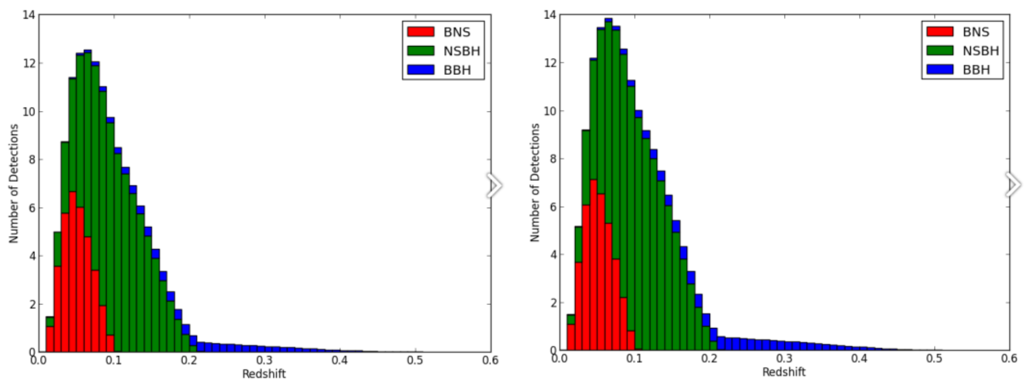

Figure 9: Plots of number of detections as a function of constant SFR (left) versus redshift dependent SFR (right)

4. ADDITIONAL RESULTS

Through these expansions to the calculator, there are also additional results that the user will receive once they have submitted their input of data. As a consequence of different mass systems being able to be selected, there is a change in presentation of results per mass system. This involves displaying individual calculations and plots that are easy to see for comparison especially since they are incorporated on the same viewing screen. The most emphasis should be placed on the newly created plot of the number of detections at each redshift because it allows the user to investigate the biases in mass systems that are detected. Samples of each of these can be seen in Figures 10-14. Please note that a figure for the merger rate as a function of redshift is not listed because the input data had a constant merger rate selected, which would just show horizontal lines on the plot.

Detection rate	125.61999999999999 per year
Detection rate BBH	8.02 per year
Detection rate BNS	34.8 per year
Detection rate NSBH	82.8 per year
Horizon redshift for BNS	0.1
Horizon redshift for BBH	0.46
Horizon redshift for NSBH	0.2
Comoving horizon distance BNS	416 Mpc
Comoving horizon distance BBH	1.76e+03 Mpc
Comoving horizon distance NSBH	814 Mpc

Figure 10: The top of the results page that the user will see after submitting their initial data.

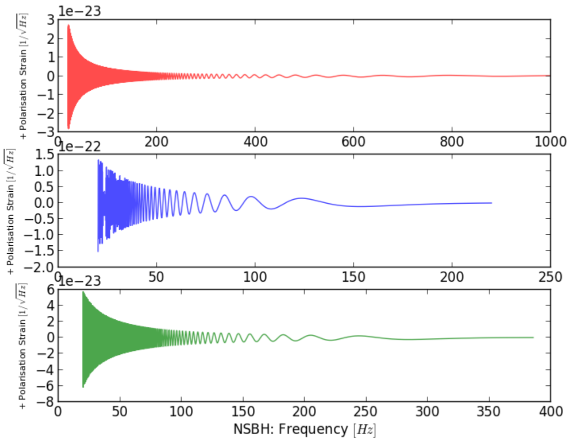

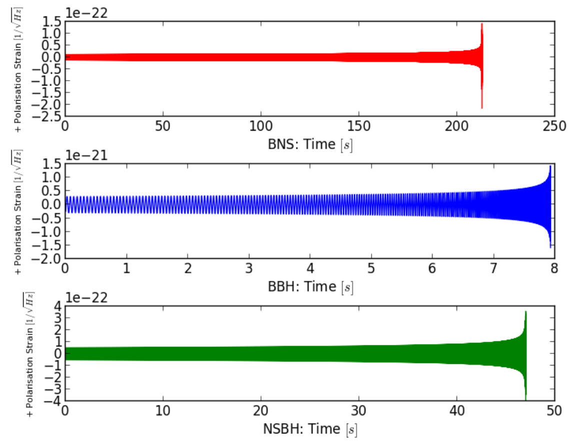

Figure 11: Sample Frequency-Domain Plots for all three mass systems

Figure 12: Sample Time-Domain Plots for all three mass systems.

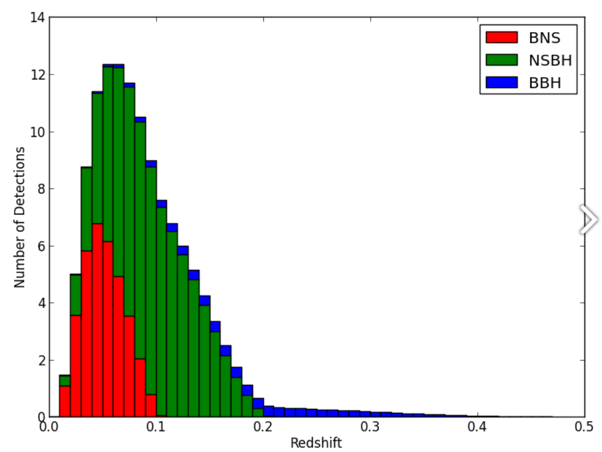

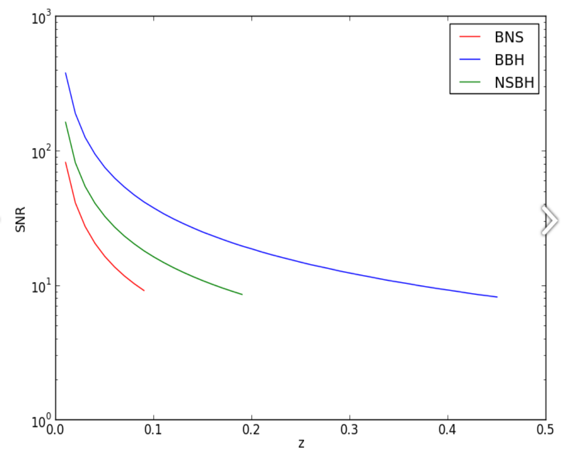

Figure 13: Sample of Number of Detections vs. Redshift

Figure 14: Sample plot of SNR vs. Redshift

DISCUSSION

This improved calculator has already provided some interesting results especially in comparison to some of the most recent published rates.[17] This comparison can be seen in using input parameters as close to the values in the publication as possible in order to test the calculator. This main difference while making this comparison is that the calculator redshifts the waveform and takes into account the cosmological effects. As seen in Figure 15, the results for BNS are quite similar, but the results for BBH are very different. This could be explained by the fact that BBHs are at farther distances so these cosmological redshift effects play more of an important role. There is current work underway to allow further investigation of these effect, which could cause a need to update these expected rates of BBHs in the aLIGO detectors.

Detection rate BBH	8.02 per year
Detection rate BNS	34.8 per year
Detection rate NSBH	82.8 per year

TABLE V: Detection rates for compact binary coalescence sources.

IFO	Source[a]	N_{low} yr^{-1}	N_{re} yr^{-1}	N_{high} yr^{-1}	N_{max} yr^{-1}
Initial	NS-NS	2×10^{-4}	0.02	0.2	0.6
	NS-BH	7×10^{-5}	0.004	0.1	
	BH-BH	2×10^{-4}	0.007	0.5	
	IMRI into IMBH			$< 0.001^{b}$	0.01^{c}
	IMBH-IMBH			$10^{-4\,d}$	$10^{-3\,e}$
Advanced	NS-NS	0.4	40	400	1000
	NS-BH	0.2	10	300	
	BH-BH	0.4	20	1000	
	IMRI into IMBH			10^{b}	300^{c}
	IMBH-IMBH			0.1^{d}	1^{e}

Figure 15: Detection rate results for SFR dependent on redshift (left) and detection rates excluding redshift effects (right). ***Please note that these CBC detection rates are not in the same order on both tables when making comparisons.

FUTURE ADDITIONS

In order to make this calculator even more realistic, there is another factor that could be accounted for. Everything within the updated calculator revolves around the idea that the parameters are dependent on redshift. In updated works being done by other scientists that we have compared our results to do no factor in these redshift effects. In order to make these comparisons on our own, this option could be incorporated for the user so then they could decide whether or not they want to include these cosmological effects. As you can see from reading the discussion, there is clearly a change in results between redshift dependent versus redshift independent. This option would allow the continuation of studying this idea more in depth.

Current work is also underway to add a graph which shows the number of detections at each SNR. This is being created because we want to know if all the detections are going to be at threshold, which is hard to do with parameter estimation, or if these detections are at higher SNRS, which is easier to do more accurate parameter estimation allowing GW sources to be further learned about.

CONCLUSION

With the hopes of GWs being detected in the near future, it is necessary to continue to better understand the type of results that could potentially be received. With the variation of many parameters and the use of up-to-date materials on this topic, the expansion of the GW even rate calculator has provided an improved way for users to make calculations, comparisons, and further exploration. The expectation is that the calculator will be live on the website by August 12, 2013, which will be a great help to the GW group not only at the University of Birmingham but also to other groups around the world as well as other persons of interest.

ACKNOWLEDGEMENTS

I would first of all really like to thank my mentor, Kat Grover, for helping me and guiding me through my summer project. I would also like to thank my advisors, Dr. Ilya Mandel and Dr. Alberto Vecchio, who provided all the materials necessary for me to have a successful summer at the University of Birmingham. I am very thankful for the University of Florida IREU Program, especially Dr. Bernard Whiting and Dr. Guido Mueller, as well as the National Science Foundation for allowing me this opportunity to grow academically, socially, culturally, and independently. I learned more than I ever expected this summer about gravitational waves, computer programming with Python, HTML, and Java Script, and I also learned what it is like to carry out a research project. All of the above will be crucial for what lies ahead in my future, and I owe it all to the people and organizations I have stated above.

---

[1] G. Harry (for the LIGO Scientific Collaboration) 2010 *Class. Quantum Grav.* **27** 084006

[2] J. Aasi *et al.* (LIGO Scientific Collaboration and Virgo Collaboration) *Phys. Rev. D 87, 022002 (2013)*

[3] C. Cutler and E. Flanagan. Phys.Rev.D49:2658-2697, 1994

[4] J. Abadie et al. (LIGO Scientific Collaboration and Virgo Collaboration) Class.Quant.Grav.27:173001, 2010

[5] G. Harry (for the LIGO Scientific Collaboration) 2010 *Class. Quantum Grav.* **27** 084006

[6]I. Mandel and R. O'Shaughnessy. *ArXiv e-prints,* 2009

[7] C. Cutler and E. Flanagan. Phys.Rev.D49:2658-2697, 1994

[8] T. Damour, B. Iyer, and B.S. Sathyaprakash. Phys.Rev. D63 (2001) 044023; Erratum-ibid. D72 (2005) 029902

[9] G. Harry (for the LIGO Scientific Collaboration) 2010 *Class. Quantum Grav.* **27** 084006

[10] I. Mandel and R. O'Shaughnessy. *ArXiv e-prints,* 2009

[11] J. Abadie et al. (LIGO Scientific Collaboration and Virgo Collaboration) Class.Quant.Grav.27:173001, 2010

[12] Ibid.

[13]Ibid.

[14] I. Mandel and R. O'Shaughnessy. *ArXiv e-prints,* 2009

[15] C.C. Steidel, K.L. Adelberger, M. Giavalisco, M. Dickinson, and M. Pettini. Astrophys.J.519:1-17, 1999

[16] V. Springel and L. Hernquist. Mon.Not.Roy.Astron.Soc. 339 (2003) 312

[17] J. Abadie et al. (LIGO Scientific Collaboration and Virgo Collaboration) Class.Quant.Grav.27:173001, 2010